

Laminar and cytoarchitectonic features of the cerebral cortex in the Risso's dolphin (*Grampus griseus*), striped dolphin (*Stenella coeruleoalba*), and bottlenose dolphin (*Tursiops truncatus*)

Rui Furutani^{1,2}

¹United Graduate School of Agricultural Science, Tokyo University of Agriculture and Technology

²Laboratory of Function and Morphology, Department of Animal Science, Utsunomiya University

Abstract

The present investigation carried out Nissl, Klüver-Barrera, and Golgi studies of the cerebral cortex in three distinct genera of oceanic dolphins (Risso's dolphin, striped dolphin and bottlenose dolphin) to identify and classify cortical laminar and cytoarchitectonic structures in four distinct functional areas, including primary motor (M1), primary sensory (S1), primary visual (V1), and primary auditory (A1) cortices. The laminar and cytoarchitectonic organization of each of these cortical areas was similar among the three dolphin species. M1 was visualized as five-layer structure that included the molecular layer (layer I), external granular layer (layer II), external pyramidal layer (layer III), internal pyramidal layer (layer V), and fusiform layer (layer VI). The internal granular layer was absent. The cetacean sensory-related cortical areas S1, V1, and A1 were also found to have a five-layer organization comprising layers I, II, III, V and VI. In particular, A1 was characterized by the broadest layer I, layer II and developed band of pyramidal neurons in layers III (sublayers IIIa, IIIb and IIIc) and V. The patch organization consisting of the layer IIIb-pyramidal neurons was detected in the S1 and V1, but not in A1. The laminar patterns of V1 and S1 were similar, but the cytoarchitectonic structures of the two areas were different. V1 was characterized by a broader layer II than that of S1, and also contained the specialized pyramidal and multipolar stellate neurons in layers III and V.

Key words cerebral cortex; dolphin; layer III-pyramidal neuron; layer V-pyramidal neuron; multipolar neuron.

Introduction

The brains of cetaceans, including whales, dolphins and porpoises, display a striking organizational difference from those of the terrestrial mammalian species (Breathnach, 1960; Morgane et al. 1985). The cetacean brains are characterized by their unique complexity of gyral and sulcal patterns (Garey et al. 1985; Glezer et al. 1988) and poor differentiation of their laminar patterns (Morgane et al. 1985). Modern whales, dolphins and porpoises have undergone a very different evolutionary history from that of the terrestrial mammalian species since they returned to an aquatic environment 70 million years ago (Kesarev et al. 1977; Gingerich et al. 1983). Most extant mammalian species demonstrate both progressive and conservative

evolutionary features (Ebner, 1969; Kirsch & Johnson, 1983). The cetacean brains exhibit peculiar features characterized by a predominance of conservative traits that are also observed in some archetypal terrestrial mammals such as echolocating bats, hedgehogs and sloths (Gerebtzoff & Goffart, 1966; Valverde & Facal-Valverde, 1986; Ferrer, 1987). Only a limited number of tract-tracing and immunohistochemical analyses have demonstrated the distribution patterns of thalamocortical afferents (Garey et al. 1989; Revishchin & Garey, 1990) and neurochemically identified neuronal populations (Revishchin & Garey, 1991; Glezer et al. 1992, 1998; Hof et al. 1992, 1995) in the cetacean cerebral cortex, in contrast to most terrestrial mammalian species (Haug, 1987; Kosaka et al. 1987; Lewis et al. 1987; Kuljis et al. 1989; Lewis, 1992). These investigational results suggest that a specific functional and immunochemically distinct neuronal population is likely to originate from morphologically distinct neuronal population and laminations. However, studies of the cetacean cerebral cortex have not included sufficient numbers of cetacean species or details focusing on the laminar organization and classification of neuronal types within the distinct functional areas. Therefore, the present study performed Nissl,

Correspondence

Rui Furutani, United Graduate School of Agricultural Science, Tokyo University of Agriculture and Technology, 350, Minemachi, Utsunomiya City, Tochigi, Japan. T: +81 28 6495436; F: +81 28 6495436; E: da051020@cc.utsunomiya-u.ac.jp

Accepted for publication 1 April 2008

Article published online 9 July 2008

Klüver-Barrera and Golgi staining of the cetacean cerebral cortex to identify and classify the laminar and cytoarchitectonic patterns of four discrete functional areas (primary motor, primary sensory, primary visual and primary auditory areas) in three oceanic dolphins including the Risso's dolphin (*Grampus griseus*), the striped dolphin (*Stenella coeruleoalba*), and the bottlenose dolphin (*Tursiops truncatus*).

Materials and methods

Animals and their brains

Three oceanic species of dolphin, Risso's dolphin ($n = 8$; *G. griseus*), striped dolphin ($n = 8$; *S. coeruleoalba*) and bottlenose dolphin ($n = 8$; *T. truncatus*), were used for the present investigation; all were female. Their brains were removed from the skull and rapidly fixed in 10% formaline for 8–12 weeks, at 4 °C. Fixed brain weights were 2113 ± 238 g (mean \pm SD; *G. griseus*), 970 ± 61 g (*S. coeruleoalba*) and 2091 ± 438 g (*T. truncatus*).

All animal experiments were carried out in accordance with the guidelines of the Animal Care and Use Committee of Utsunomiya University. All efforts were made to minimize animal suffering and to reduce the number of animals used.

Brain regions

Four distinct functional cortical areas were examined, including primary motor cortex (M1), primary sensory cortex (S1), primary visual cortex (V1) and primary auditory cortex (A1), as identified by Supin and his colleagues (1977, 1978). Cytoarchitectonic studies were performed in the anterior-cruciate gyrus (for M1), posterior-cruciate and coronary gyri (for S1), lateral gyrus (for V1), and the suprasylvian gyrus (for A1) of the cerebral cortex.

Histology

Nissl and Klüver-Barrera methods

To evaluate and classify laminar and cytoarchitectonic features of the cetacean cortex, six brains from each of the three dolphin species were embedded in paraffin. Serial sections were cut in the coronal plane (20 μ m thickness), and divided into two series. One series was stained with 0.1% cresyl violet (Nissl staining) and the other using the Klüver-Barrera method (Klüver & Barrera, 1953). Stained sections were evaluated under the light microscope. Laminar patterns were identified and classified in each of the functional areas and laminar thicknesses were measured using computer-aided analysis of video images (NIH Image 1.61; National Institutes of Health) viewed with a microscope (BX 50, Olympus, Tokyo). Measurements of each layer of the four discrete cortical areas were carried out in every 18th section (360 μ m apart) per animal ($n = 6$). Measurements are expressed as means \pm SD. Student's *t* test was used to assess the statistical significance of the differences between means in different cortical layers in the same specimen and between the same layers in different specimens.

Golgi method

Two brains from each of the three dolphin species were impregnated with a tungstate modification of the Golgi-Cox method (Ramon-Moliner, 1958). The brains were placed in the fixative for 20 days, alkalized for 24 h, soaked for 24 h in two changes of

0.05% acetic acid, and then washed with distilled water. After dehydration in ethanol, they were embedded in paraffin. Serial sections were cut in the coronal plane (100–150 μ m thickness). Golgi-impregnated sections were used to classify the neuronal types composing each layer of the discrete cortical areas, focusing on such anatomical elements as somatic shape and size, number of primary dendrites, and dendritic orientation. The soma size (short axis and long axis of soma) was measured using computer-aided analysis of video images (NIH Image 1.61, National Institutes of Health) viewed with a microscope (BX 50, Olympus, Tokyo). Measurements are expressed as means \pm SD.

Results

The laminar patterns and cytoarchitectonic organizations were different in the four areas examined in the present study (Table 1). In particular, the thicknesses of the molecular and external granular layers could be used to characterize anatomically the four distinct cortical areas examined (Table 1).

Primary motor cortex (M1)

M1 of the Risso's dolphin, striped dolphin, and bottlenose dolphin displayed similar laminar patterns (Fig. 1A–C) that included a molecular layer (layer I), external granular layer (layer II), external pyramidal layer (layer III), internal pyramidal layer (layer V) and fusiform layer (layer VI). An internal granular layer (layer IV) was not detected in M1. Layer II was narrow, but densely packed with small granular (short axis: 12 ± 5 μ m, long axis: 19 ± 6 μ m) and pyramidal neurons (short axis: 22 ± 3 μ m, long axis: 26 ± 2 μ m). Layer V contained large pyramidal neurons (short axis: 38 ± 8 μ m, long axis: 67 ± 11 μ m; Fig. 1D–F). Layer VI contained small bipolar (short axis: 9 ± 4 μ m, long axis: 13 ± 6 μ m) and triangular neurons (short axis: 17 ± 3 μ m, long axis: 30 ± 4 μ m).

Primary sensory cortex (S1)

The laminar organization of S1 was similar across the three dolphin species (Fig. 2A–F) and was also found to be a five-layer structure comprising the layers I, II, III, V and VI (Fig. 2A–C). Layer IV was not detected in S1. Layers I and II were broader than those of M1, but a significant difference was detected between layer II of M1 and S1 ($P < 0.05$) (Table 1). Layer I contained few cell bodies, and layer II was found to have nonpyramidal and pyramidal neurons. Layer III was observed as a richly developed layer and could be divided into three discrete sublayers (layers IIIa, IIIb and IIIc) based on the anatomical boundaries between each sublayer (Fig. 2A–F). Of these, layers IIIa and IIIc were particularly well developed in the S1. The neuronal mass expressed a patch-like distribution in layer IIIb (Fig. 2A–C). Layers III and V comprised pyramidal neurons, increasing in size with depth (Fig. 2D–F). The dendritic trees of its neurons were well developed. The largest pyramidal

Table 1 Laminar thicknesses of various cetacean cortical areas

Thickness (µm): mean ± SD		Risso's dolphin			Striped dolphin			Bottlenose dolphin					
Layer		M1	S1	V1	A1	M1	S1	V1	A1	M1	S1	V1	A1
I		300 ± 26	338 ± 10	330 ± 26	433 ± 75	230 ± 44	263 ± 104	283 ± 40	380 ± 78	313 ± 31	328 ± 19	311 ± 45	367 ± 58
II		89 ± 9	215 ± 23	222 ± 31	258 ± 54	133 ± 25	160 ± 40	225 ± 31	227 ± 23	107 ± 15	172 ± 43	193 ± 23	230 ± 46
III		343 ± 35	380 ± 35	398 ± 24	493 ± 67	340 ± 17	413 ± 76	406 ± 21	417 ± 25	327 ± 12	403 ± 59	413 ± 49	423 ± 18
V		483 ± 14	353 ± 40	350 ± 53	343 ± 15	360 ± 17	377 ± 35	357 ± 25	340 ± 20	416 ± 46	305 ± 61	340 ± 20	363 ± 42
VI		520 ± 106	507 ± 61	523 ± 51	517 ± 50	490 ± 131	467 ± 45	537 ± 91	483 ± 51	460 ± 79	520 ± 44	507 ± 32	467 ± 35
Total		1735 ± 113	1793 ± 108	1824 ± 112	2045 ± 191	1553 ± 72	1680 ± 277	1808 ± 112	1847 ± 160	1623 ± 55	1728 ± 108	1764 ± 92	1850 ± 15

M1, primary motor cortex; S1, primary sensory cortex; V1, primary visual cortex; A1, primary auditory cortex.

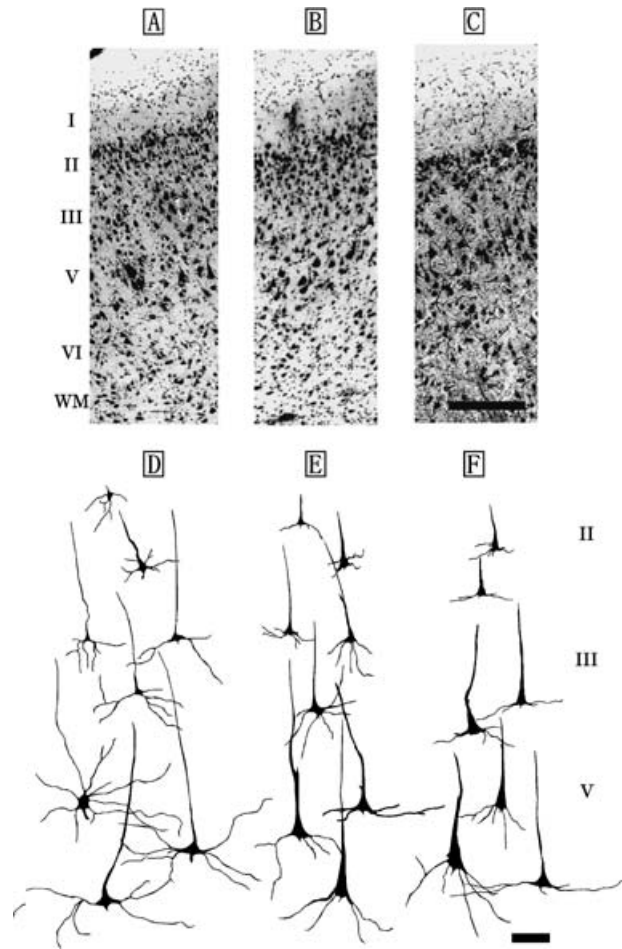


Fig. 1 Photomicrographs of Nissl-stained, coronal sections of primary motor area (M1) in the Risso's dolphin (A), striped dolphin (B), and bottlenose dolphin (C). Scale bar indicates 300 µm (A–C). Schematic drawings represent Golgi-impregnated neurons of layers II, III, and V in M1 of the Risso's dolphin (D), striped dolphin (E) and bottlenose dolphin (F). Scale bar indicates 100 µm (D–F). I: layer I (molecular layer); II: layer II (external granular layer); III: layer III (external pyramidal layer); V: layer V (internal pyramidal layer); VI: layer VI (fusiform layer); WM: white matter.

neurons (short axis: $23 \pm 9 \mu\text{m}$, long axis: $52 \pm 12 \mu\text{m}$) in S1 were found in layer V (Fig. 2D–F). Layer VI was detected to have nonpyramidal neurons such as bipolar and triangular neurons.

Primary visual cortex (V1)

The laminar patterns and cytoarchitectonic structures of V1 were similar across the three dolphin species (Fig. 3A–C). V1 was organized in five layers, consisting of the layers I, II, III, V and VI (Fig. 3A–C). Layer IV was not detected in V1. Layer II was densely packed with small bipolar and pyramidal neurons (Fig. 5A), and it was broader than that found in S1, although it did not differ significantly from that of S1 (Table 1). Layer III was also observed as a richly developed laminar structure that could be classified into

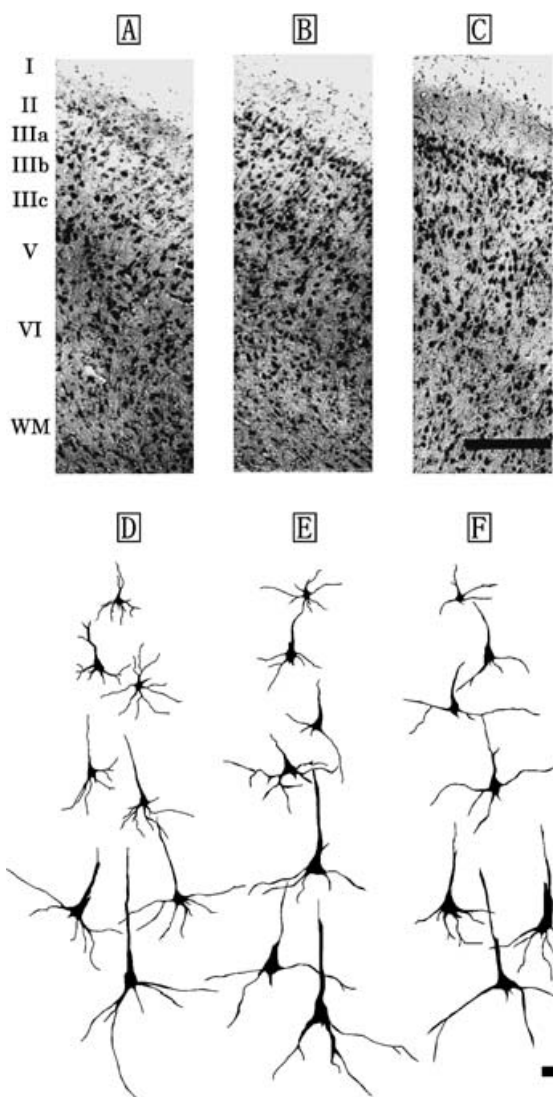


Fig. 2 Photomicrographs of Nissl-stained, coronal sections of primary sensory area (S1) in the Risso's dolphin (A), striped dolphin (B), and bottlenose dolphin (C). Scale bar indicates 300 μm (A–C). Schematic drawings represent Golgi-impregnated neurons of layers II, III, and V in S1 of the Risso's dolphin (D), striped dolphin (E), and bottlenose dolphin (F). Scale bar indicates 100 μm (D–F). I: layer I; II: layer II; III: layer III consisted of the three discrete sublayers IIIa, IIIb and IIIc; V: layer V; VI: layer VI; WM: white matter.

three discrete sublayers, IIIa, IIIb, and IIIc, based on the anatomical boundaries between each sublayer (Fig. 3A–C). Layers IIIa and IIIc were particularly well developed in V1. Layer IIIb of V1 contained the patches consisting of the layer IIIb-pyramidal neurons (Fig. 3A–C, Fig. 5B). A similar cytoarchitectonic organization of layer III was detected in both S1 (Fig. 2A–C) and V1 (Fig. 3A–C), whereas layer V of V1 was different from that of S1 (Fig. 2D–F) due to the presence of large pyramidal neurons (short axis: $29 \pm 7 \mu\text{m}$, long axis: $63 \pm 12 \mu\text{m}$) indicating a thick apical dendrite in V1 (Fig. 3D–F). These layer V pyramidal neurons (Fig. 5C) had larger somata, and longer and thicker apical dendrites

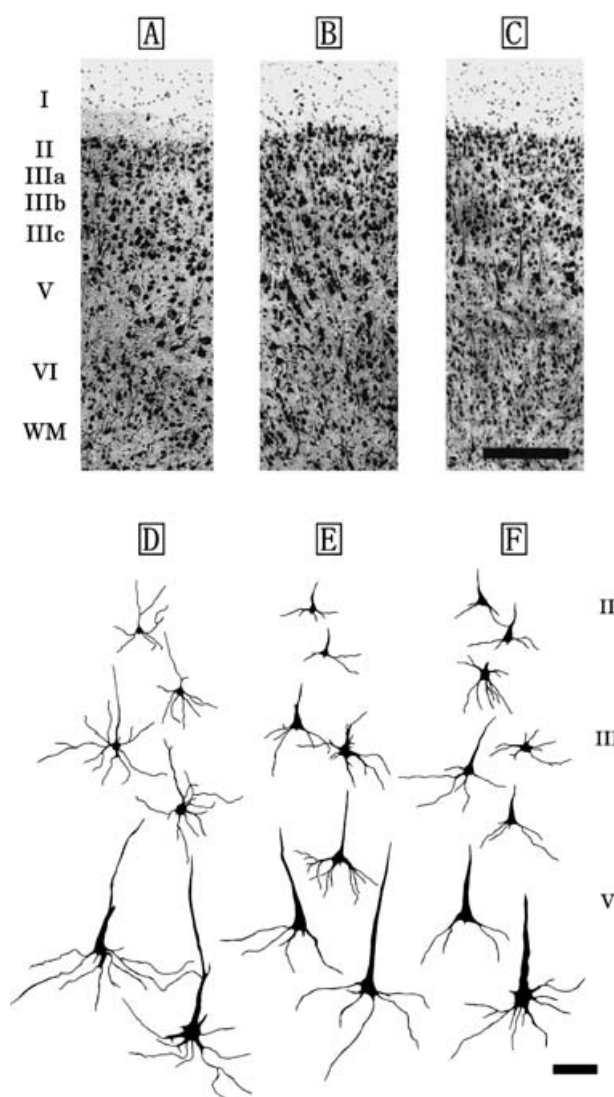


Fig. 3 Photomicrographs of Nissl-stained coronal sections of the primary visual area (V1) in the Risso's dolphin (A), striped dolphin (B), and bottlenose dolphin (C). Scale bar indicates 300 μm (A–C). Schematic drawings represent Golgi-impregnated neurons of layers II, III, and V in V1 of the Risso's dolphin (D), striped dolphin (E) and bottlenose dolphin (F). Scale bar indicates 100 μm (D–F). I: layer I; II: layer II; III: layer III consisted of the three discrete sublayers IIIa, IIIb and IIIc; V: layer V; VI: layer VI; WM: white matter.

than those found in S1 (Fig. 2D–F). Large multipolar stellate neurons (short axis: $37 \pm 16 \mu\text{m}$, long axis: $44 \pm 8 \mu\text{m}$; Fig. 5D) were detected in the lower portion of layer III and layer V of V1. Layer VI was found to have bipolar and triangular neurons.

Primary auditory cortex (A1)

The A1 cortical area was also found to have a five-layer organization consisting of layers I, II, III, V and VI (Fig. 4A–C) in the three dolphin species. Layers I and II were thicker in A1 than in all other cortical areas examined, but did not

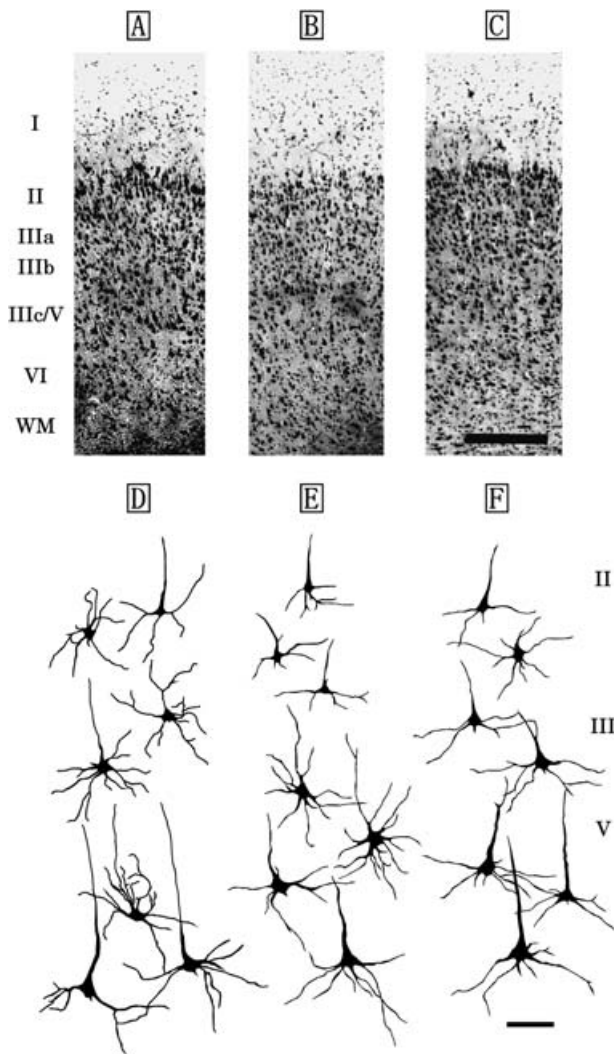


Fig. 4 Photomicrographs of Nissl-stained coronal sections of primary auditory area (A1) in the Risso's dolphin (A), striped dolphin (B), and bottlenose dolphin (C). Scale bar indicates 300 μm (A–C). Schematic drawings represent Golgi-impregnated neurons of layers II, III, and V in A1 of the Risso's dolphin (D), striped dolphin (E) and bottlenose dolphin (F). Scale bar indicates 100 μm (D–F). I: layer I; II: layer II; III: layer III consisted of the three discrete sublayers IIIa, IIIb and IIIc; V: layer V; VI: layer VI; WM: white matter.

differ significantly from those of S1 and V1 (Table 1). Layer II of A1 was significantly broader than that of M1 ($P < 0.05$). A1 contained a layer IIIa, IIIb with mostly pyramidal neurons, fusion of the lower portion of layer III and layer V constituting a combined layer IIIc/V (Fig. 4A–C). Layers IIIa and IIIb were more densely packed with cells in A1 (Fig. 4A–C) than those detected in S1 (Fig. 2A–C) and V1 (Fig. 3A–C). Layer IIIc/V contained large pyramidal neurons (short axis: $27 \pm 2 \mu\text{m}$, long axis: $59 \pm 8 \mu\text{m}$), and multipolar stellate neurons (short axis: $30 \pm 9 \mu\text{m}$, long axis: $42 \pm 4 \mu\text{m}$) with 5–7 primary dendrites. Cells of layer V of A1 were denser than those detected in S1 and V1. Layer VI was found to have small bipolar and triangular neurons. Layer IV was

not detected in the region between layers IIIc and V. The laminar and cytoarchitectonic structures of A1 were similar across the three dolphin species examined (Fig. 4A–F).

Discussion

The organization of the cerebral cortices was similar in laminar patterns and layer-specific cytoarchitectonic structures across the three dolphin species, *G. griseus*, *S. coerulealba*, and *T. truncatus*. At the same time, there were area-specific characteristics within the four distinct functional areas (M1, S1, V1 and A1) of the three dolphin species. In general, the cetacean neocortex was thin, its overall pattern of lamination was not well expressed, and it contained a thick molecular layer (layer I). Areas S1, V1, and A1 of the three dolphin species displayed different laminar patterns from those of terrestrial mammalian species (Haug, 1987). These cetacean sensory-related cortical areas have a five-layer organization, including layers I, II, III, V and VI, and the absence of an internal granular layer (layer IV), whereas those of rodents (Haug, 1987) and primates (Haug, 1987; Lewis, 1992) are six-layer structures that include a well-developed layer IV. In these species, layer IV is the major input layer for thalamocortical-specific afferents, and is seen as a well-expressed granularization (Haug, 1987; Lewis, 1992). Histochemical studies of cytochrome oxidase (CO) have shown that the thalamoreceptive layer IV of the visual cortex is densely stained for CO in cats (Wong-Riley, 1979; Wong-Riley & Carroll, 1984), whereas in the bottlenose dolphin and harbour porpoise the visual and auditory regions are most noticeably characterized by two stripes of dark CO staining, one in the upper half of layer I and the other in layer III (Revishchin & Garey, 1990). These reports suggest that cetacean sensory areas might receive afferent inputs from thalamus via layers I and III without layer IV. Moreover, layers I, II and III contain a very high percentage of GABA-positive neurons in V1 of the Black Sea porpoise (Garey et al. 1989). In the cat visual area, the high percentage of GABA-positive neurons is localized in the layers IV and lower III, where most thalamocortical axons terminate (Gabbott & Somogyi, 1986). Some tract-tracing and immunohistochemical analyses have demonstrated that thalamocortical afferents of the cetacean cerebral cortex are distributed in layers I, II and III, and that most axons terminate in layer III (Garey et al. 1989; Revishchin & Garey, 1990, 1991; Glezer et al. 1992, 1998) in contrast to most terrestrial mammalian species (Haug, 1987; Kosaka et al. 1987; Lewis et al. 1987; Kuljis et al. 1989; Lewis, 1992).

The present results demonstrate that sensory-related cortical areas such as S1, V1, and A1 all display an absence of layer IV and a general lack of granularization in the three dolphin species. An 18-day-old brain of *T. truncatus* shows signs of immaturity in its visual cortex, and also a distinct granular band occurs between layers III and V and

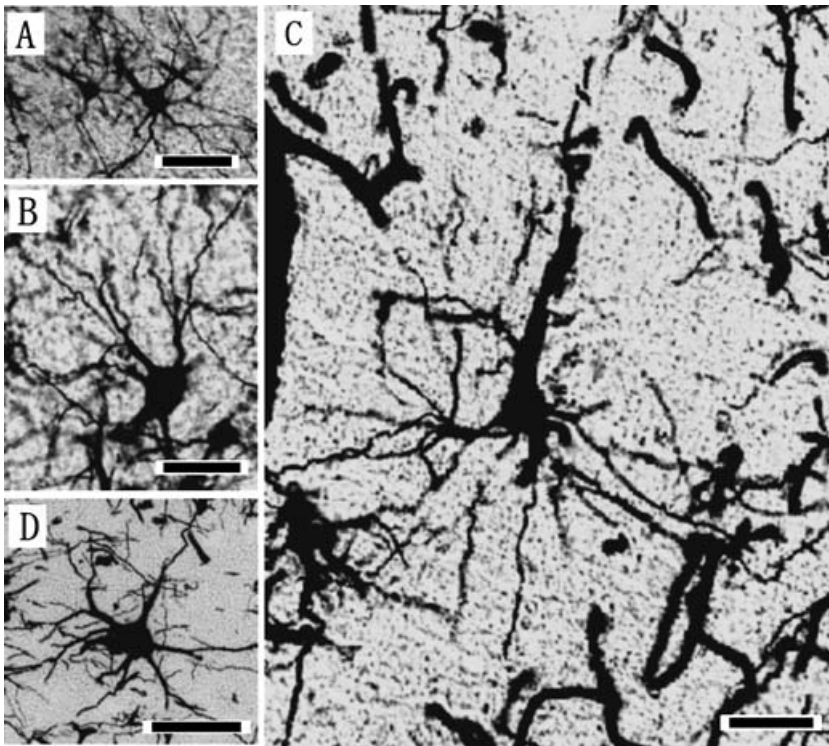


Fig. 5 Photomicrographs of the Golgi-impregnated pyramidal neurons in layers II (A), IIIb (B), V (C), and multipolar (D) neurons of layer IIIc in the coronal sections of primary visual area (V1) in the Risso's dolphin. Scale bars indicate 25 μm (A, B) and 50 μm (C, D).

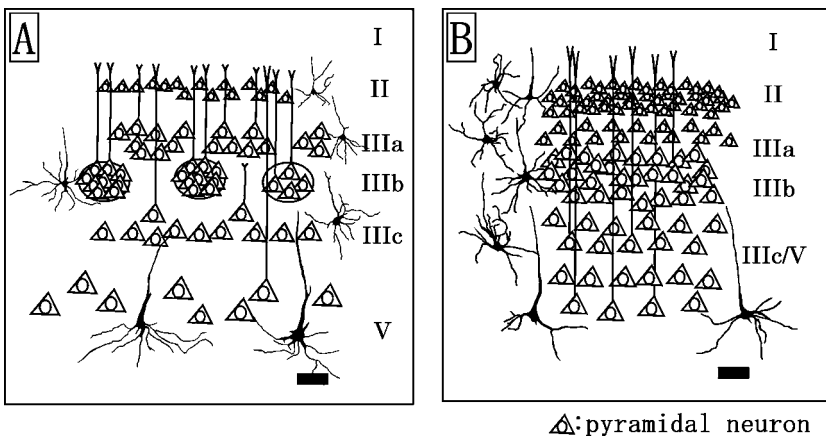


Fig. 6 Schematic drawings represent the distribution patterns of pyramidal neurons of the primary visual (A) and primary auditory (B) cortices in the dolphin species. Scale bars indicate 100 μm (A and B).

seems to be a rudimentary layer IV (Garey et al. 1985). At 3 years of age most adult features have developed, but layer IV is still detectible (Garey et al. 1985). The bottlenose dolphins (*T. truncatus*) used in the present study were adult females and their fixed brain weight was larger (2091 ± 438 g) than those used in the previous investigation (Garey et al. 1985). Thus, layer IV was not detected in V1 in the present study. Instead, the sensory-related cortices including S1, V1 and A1 are characterized by area- and layer-specific differences exhibited in 1) the thicknesses of layers I, II and III, 2) the morphology of the pyramidal and multipolar stellate neurons in layers III and V, and 3) the cytoarchitecture in the sublayers IIIa, IIIb and IIIc (presence or absence of the patch organizations consisted of layer IIIb-pyramidal neurons). S1 and V1 (Fig. 6A) contained the

patches of the layer IIIb-neurons, whereas the layer IIIb of A1 (Fig. 6B) was detected as a continuous neuronal band without anatomical blank between cell populations in the present study. The occurrence of apical dendritic bundles arising from pyramidal neurons in layers III and V has been reported in several neocortical areas and further suggested that these may be a general feature of cortical organization (Fleischhauer et al. 1972). The bundles of apical dendrites originating from the layer III- and V-pyramidal neurons concentrate in layer I, and form an area-specific honeycomb mosaic (Ichinohe et al. 2003). An interesting possibility is that the patches of layer IIIb-pyramidal neurons of S1 and V1 reported here may contribute to construct a different shape and size of bundles of apical dendrites from those of A1. The lamination in V1 is similar to that in S1;

however, the layer V-pyramidal neurons in V1 have larger somata and longer and thicker apical dendrites than those in S1 in the three dolphin species. The thicknesses of layers II and III of V1 are broader than those of S1 in the three dolphin species examined. This suggests also that the apical dendritic bundles arising from layer V-pyramidal neurons of V1 might constitute a distinct type from those of S1. Cetacean sensory cortices contain layer I that is much thicker than those of terrestrial mammalian species (Haug, 1987; Lewis, 1992). Layers I and II of A1 were the thickest in all cortical areas examined. Layer I in many areas receives cortical feedback and thalamocortical connections, and amygdalo-cortical projections terminate widely at the border of layers I and II (Amaral & Price, 1984; Stefanacci et al. 1996). Those anatomical differences between the distinct sensory-related cortices (S1, V1 and A1) may stem from the functional specificity of each cortex. The lateral geniculate nucleus projects to the visually excitable part of V1 (Krasnoshchekova & Figurina, 1980; Revishchin & Garey, 1990), and also dense CO-staining exists in layer III of V1 (Revishchin & Garey, 1991). Calcium-binding protein (CaBP)-immunoreactive neurons, including calretinin (CR)-, calbindin (CB)-, and parvalbumin (PV)-immunoreactive neurons, are distributed in the upper layers II and III in the cetacean visual cortex (Glezer et al. 1992, 1993, 1998). Thus, V1 of the oceanic dolphin species including the Risso's dolphin, striped dolphin and bottlenose dolphin might contain well-developed layers II and III.

Thalamocortical afferents from the medial geniculate nucleus terminate in the primary auditory area (Revishchin & Garey, 1990). In the echolocating dolphin species examined in the present study, A1 displays a well-developed layer III; in particular, the bands of pyramidal neurons within layers IIIa, IIIb, IIIc, and V are the broadest of the cortical areas examined. There are also differences in the distribution of CaBP-immunoreactive neuronal populations between A1 and V1 (Glezer et al. 1992). The highest densities of CR- and CB-immunoreactive neurons exist in layers I and II, whereas PV-immunoreactive neurons exist mostly in layers IIIc/V (Glezer et al. 1998). The morphology of PV-immunoreactive neurons is similar to that of multipolar stellate neurons detected in layers IIIc/V in the present study.

The dolphin cerebral cortex has a large surface area, but it is not particularly thick in relation to brain weight. Nevertheless, lamination is distinct in each of four cortical areas (M1, S1, V1 and A1). These results suggest that morphologically different laminar patterns and cytoarchitectonic structures (such as somatic shape, size, dendritic pattern, and orientation of the apical dendrites of multipolar neurons, layer III- and V-pyramidal neurons) in distinct layers and areas, correspond to specific functional differences, and their histological profiles also join the construction of the morphologically distinct bundles of apical dendrites that receive the area-specific cortical feedback and thalamocortical connections.

Acknowledgements

The author is grateful to Professor Shoei Sugita of Utsunomiya University, Utsunomiya, for his help in making this study possible. The author wishes to thank Dr. Toshihide Iwasaki for fresh tissue contributions. Special thanks are given to the National Research Institute of Far Seas Fisheries, and Japan Fisheries Cooperative of Taiji for fresh tissue contributions.

References

- Amaral DG, Price JL (1984) Amygdalo-cortical projections in the monkey (*Macaca fascicularis*). *J Comp Neurol* **230**, 465–496.
- Breathnach AS (1960) The cetacean nervous system. *Biol Rev* **35**, 187–230.
- Ebner FF (1969) A comparison of primitive forebrain organization in metatherian and eutherian mammals. *Ann NY Acad Sci* **167**, 241–257.
- Ferrer I (1987) The basic structure of the neocortex in the insectivorous bats (*Miniopterus threibershi* and *Pipistrellus pipistrellus*). A Golgi study. *J Hirnforsch* **28**, 237–243.
- Fleischhauer K, Petsche H, Wittkowski W (1972) Vertical bundles of dendrites in the neocortex. *Z Anat Entwicklungsgesch* **136**, 213–223.
- Gabbott PLA, Somogyi P (1986) Quantitative distribution of GABA-immunoreactive neurons in the visual cortex (area 17) of the cat. *Exp Brain Res* **61**, 323–331.
- Garey LJ, Takacs J, Revishchin AV, Hamori J (1989) Quantitative distribution of GABA-immunoreactive neurons in cetacean visual cortex is similar to that in land mammals. *Brain Res* **485**, 278–284.
- Garey LJ, Winkelmann E, Brauer K (1985) Golgi and Nissl studies of the visual cortex of the bottlenose dolphin. *J Comp Neurol* **240**, 305–321.
- Gerebtzoff MA, Goffart M (1966) Cytoarchitectonic study of the isocortex in the sloth (*Choloepus hoffmanni* Peters). *J Comp Neurol* **126**, 523–534.
- Gingerich PD, Welis NA, Russel NA, Shah SM (1983) Origin of whales in epicontinental remnant seas: new evidence from early Eocene of Pakistan. *Science* **220**, 403–406.
- Glezer II, Hof PR, Leranch C, Morgane PJ (1993) Calcium-binding protein-containing neuronal populations in mammalian visual cortex: a comparative study in whales, insectivores, bats, rodents, and primates. *Cereb Cortex* **3**, 249–272.
- Glezer II, Hof PR, Morgane PJ (1992) Calretinin-immunoreactive neurons in the primary visual cortex of dolphin and human brains. *Brain Res* **595**, 181–188.
- Glezer II, Hof PR, Morgane PJ (1998) Comparative analysis of calcium-binding protein-immunoreactive neuronal populations in the auditory and visual systems of the bottlenose dolphin (*Tursiops truncatus*) and the macaque monkey (*Macaca fascicularis*). *J Chem Neuroanat* **15**, 203–237.
- Glezer II, Jacobs MS, Morgane PJ (1988) The 'initial' brain concept and its implication for brain evolution in cetacea. *Behav Brain Sci* **11**, 75–116.
- Haug H (1987) Brain size, surface and neuronal size of the cortex cerebri. A stereological investigation of man and his variability and a comparison with some mammals (primates, whales, marsupialia, insectivores and one elephant). *Am J Anat* **180**, 126–142.
- Hof PR, Glezer II, Archin N, Janssen WG, Morgane PJ, Morrison JH (1992) The primary auditory cortex in cetacean and human brain: a comparative analysis of neurofilament protein-containing pyramidal neurons. *Neurosci Lett* **146**, 91–95.

- Hof PR, Glezer II, Revishchin AV, Bouras C, Charnay Y, Morgane PJ** (1995) Distribution of dopaminergic fibers and neurons in visual and auditory cortices of harbor porpoise and pilot whale. *Brain Res Bull* **36** (3), 275–284.
- Ichinohe N, Fujiyama F, Kaneko T, Rockland K** (2003) Honeycomb-like mosaic at the border of layers 1 and 2 in the cerebral cortex. *J Neurosci* **23**, 1372–1382.
- Kesareve VS, Malofeyeva LI, Trykova OV** (1977) Echological specificity of cetacean neocortex. *J Hirnforsch* **18**, 447–460.
- Kirsch JAW, Johnson JI** (1983) Phylogeny through brain traits: Trees generated by neural characters. *Brain Behav Evol* **22**, 60–69.
- Klüver H, Barrera E** (1953) A method for the combined staining of cells and fibers in the nervous system. *J Neuropathol Exp Neurol* **12**, 400–406.
- Kosaka T, Kosaka K, Hataguchi Y, et al.** (1987) Catecholaminergic neurons containing GABA-like and/or glutamic acid decarboxylase-like immunoreactivities in various brain regions of the rat. *Exp Brain Res* **66**, 191–210.
- Krasnoshchekova EI, Figurina II** (1980) Cortical projections of the dolphin cerebral geniculate body. *Arkh Anat Gistol Embriol* **78**, 19–24.
- Kuljis RO, Martin-Vasallo P, Peress NS** (1989) Lewy bodies in tyrosine hydroxylase-synthesizing neurons of the human cerebral cortex. *Neurosci Lett* **106**, 49–54.
- Ladygina TF, Supin AY** (1977) Localization of the sensory projection areas in the cortex of the dolphins. *Zh Evol Biokhim Fiziol* **13**(6), 712–718.
- Lewis DA** (1992) The catecholaminergic innervation of primate prefrontal cortex. *J Neural Transm Suppl* **36**, 179–200.
- Lewis DA, Campbell MJ, Foote SL, Goldstein M, Morrison JH** (1987) The distribution of tyrosine hydroxylase-immunoreactive fibers in the primate neocortex is widespread but regionally specific. *J Neurosci* **7**, 279–290.
- Morgane PJ, Jacobs MS, Galaburda AM** (1985) Conservative features of neocortical evolution. *Brain Behav Evol* **26**, 176–184.
- Ramon-Moliner E** (1958) A tungstate modification of the Golgi Cox method. *Stain Technol* **33**, 19–29.
- Revishchin AV, Garey LJ** (1990) The thalamic projection to the sensory neocortex of the porpoises, *Phocoena phocoena*. *J Anat* **169**, 85–102.
- Revishchin AV, Garey LJ** (1991) Laminar distribution of cytochrome oxidase staining in cetacean isocortex. *Brain Behav Evol* **37**, 355–367.
- Stefanacci L, Suzuki WA, Amaral DG** (1996) Organization of connections between the amygdaloid complex and the perirhinal and parahippocampal cortices in the macaque monkeys. *J Comp Neurol* **375**, 552–582.
- Supin AY, Mukhametov LM, Ladygina TF, Popov VV, Mass AM, Poliakova IG** (1978) Neurophysiologic characteristics of the cetacean cerebral cortex in dolphins. In *Electrophysiological Study of the Dolphin Brain* (in Russian), pp. 29–85. Moscow: Izdatel'ato Nauka.
- Valverde F, Facal-Valverde MV** (1986) Neocortical layers I and II of the hedgehog (*Erinaceus europaeus*): I. Intrinsic organization. *Anat Embryol* **173**, 413–430.
- Wong-Riley M** (1979) Changes in the visual system of monocularly sutured or enucleated cats demonstrable with cytochrome oxidase histochemistry. *Brain Res* **171**, 11–28.
- Wong-Riley M, Carroll EW** (1984) Effects of impulse blockage on cytochrome oxidase activity in monkey visual system. *Nature* **307**, 262–264.